The beviour of cracks in plain and reinforced concrete subjected to shear

Autor(en): **Walraven, Joost C.**

Objekttyp: **Article**

Zeitschrift: **IABSE reports of the working commissions = Rapports des commissions de travail AIPC = IVBH Berichte der Arbeitskommissionen**

Band (Jahr): **34 (1981)**

PDF erstellt am: **22.05.2024**

Persistenter Link: https://doi.org/10.5169/seals-26890

The Behaviour of Cracks in Plain and Reinforced Concrete Subjected to Shear

Le comportement des fissures en béton armé et non armé

Das Verhalten von Rissen in bewehrtem und unbewehrtem Beton

JOOST C. WALRAVEN
Dr. ir., Research engineer
Stevin Laboratory, Delft University of Technology,
Delft, The Netherlands

SUMMARY
Due to the roughness of their surfaces, cracks in concrete can transmit substantial shear forces. Constitutive equations are derived for cracks in plain and reinforced concrete on the basis of a realistic description of the physical behaviour, in such a way that the influence of the concrete mix properties can be taken into account.
Comparisons between theoretical and experimental results are presented. Bearing capacities are derived for cracks in plain concrete under different loading conditions and for cracks in reinforced concrete subjected to pure shear loading. Comparisons are made with existing shear-friction equations.

RÉSUMÉ
Suite à la rugosité de leurs surfaces, les fissures dans le béton ont la possibilité de transmettre des efforts tranchants considérables. Des rélations entre les contraintes et les déplacements sont données pour des fissures en béton armé et non armé, sur base d'une description réaliste du comportement physique, de telle manière qu'il est possible de tenir compte de l'influence des propriétés du béton.
Des comparaisons sont établies entre les résultats théoriques et expérimentaux. Les résistances sont données pour des fissures en béton non-armé, soumises à des sollicitations différentes et pour des fissures en béton armé soumises au cisaillement pur.

ZUSAMMENFASSUNG
Infolge der Rauhigkeit ihrer Rissufer können Risse im Beton beträchtliche Schubkräfte übertragen. Die Beziehungen zwischen Spannungen und Verschiebungen sind auf der Grundlage einer wirklichkeitsnahen Beschreibung des Materialverhaltens für Risse in unbewehrtem und bewehrtem Beton abgeleitet, derart dass auf den Einfluss der Betonzusammensetzung Rücksicht genommen werden kann. Theoretische und experimentelle Ergebnisse sind verglichen.
Die Tragfähigkeit von Rissen in unbewehrtem Beton unter verschiedenen Beanspruchungsarten und von Rissen in bewehrtem Beton unter reiner Schubbeanspruchung ist abgeleitet.

1. INTRODUCTION

In many concrete structures the capacity of cracks to transmit shear forces plays an important role. Cracks, which have been formed due to flexural action, may be subjected to shear forces as a result of other loading configurations. Such a situation occurs for instance in a long bridge, which is supported on hinged columns in the longitudinal axis, so that the torsional moments have to be resisted by the abutments. In such a case open cracks have to be able to transmit shear forces, to warrant the full load bearing capacity. In the design of nuclear power vessels the behaviour of cracks subjected to shear loading is directly taken into account. Design criteria [1] require that the structure be designed to withstand the simultaneous occurence of an internal pressurization, so that horizontal and vertical cracks are formed, and the inertia forces generated by a strong motion earthquake.

The variation of external loading conditions is not a necessary condition for the occurence of shear forces in cracks. The anisotropic properties of cracked reinforced concrete may as well cause shear action in the cracks. The shear capacity of beams without shear reinforcement depends essentially on the resistance of the cracks against shear displacements [2,3,4].
Up to now the understanding of what really happens in a crack subjected to shear forces was not satisfactory. Examples of some frequently encoutered simplifications are shown in Fig. 1a,b. In Fig. 1a the whole mechanism is reduced to the case of simple friction between two interfaces ($\tau = \mu.\sigma$). Fig. 1b considers the possibility of crack dilatancy. If the undulations of the crack faces are considered to be rigid and frictionless, the mechanism can be described by a similar relation τ = (tang. ϕ) σ. If the undulations are considered as elastic a description is more difficult: during shear displacement at constant crack width both a shear stress τ and a normal stress σ are developed. Further complications occur if it is assumed that the undulations are not perfectly elastic and frictionless. Due to all these incertainties only provisional equations were available for the use in non linear finite element programs, so that even the most advanced programs could not be used with full profit.
It was concluded that there is a need for a better understanding of the phenomenon, improved constitutive equations and better defined strength limits. This paper focusses on these questions. The work was carried out within the scope of the project "Concrete Mechanics" supported by the CUR-VB, the Netherlands Committee of Concrete Research.

2. CONSTITUTIVE EQUATIONS

2.1 Cracks in plain concrete

In order to obtain constitutive equations with a wide range of applicability it is necessary to describe the physical reality as accurate as possible. Hence first the fundamental behaviour is studied.
In general the strength and the stiffness of the aggregate particles are higher than those of the matrix, consisting of hardened cement paste and small particles (f.i. < 0.1 mm). The contact area between the two materials, the bond zone, is the weakest link of the system. Hence, cracking occurs commonly through the matrix, but along the circumference of the aggregate particles. Only in the case of high strength concretes (with high matrix strength) and lightweight concrete (with low particle strength) are cracks observed running both through the ma-

trix and the particles. Generally crack faces are encountered which have a structure as indicated in Fig. 2.

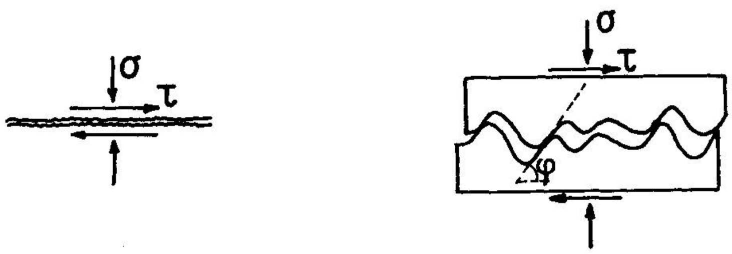

Fig. 1 a, b. Simplified representation of crack behaviour

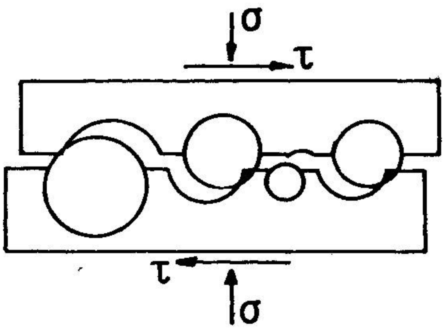

Fig. 2. More realistic representation of crack behaviour

It can be expected that, during shear displacement of the crack faces, contact areas develop on the surface of the particles exceeding from one of the crack faces. The behaviour in detail, for a single particle, is represented in Fig. 3.

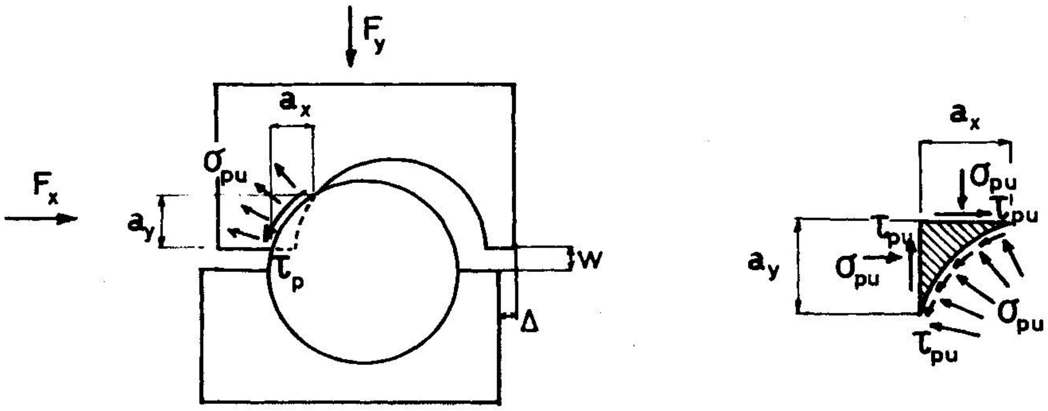

Fig. 3a. Formation of a contact area b. Equilibrium at a contact area

If the shear stress τ on the plane of cracking is increased and crack opening is counteracted by a restraining stress σ , a mechanism will develop, which can be described as follows: the contact areas tend initially to slide: as a result of this sliding, the contact areas are reduced, which results in high contact stresses, so that further deformation occurs. Hardened cement paste is a visco-elastic material: the deformation, provoked by stresses is only partially elastic, for the other part plastic. Under multi-axial stresses, as in the area between the aggregate particles in concrete, large plastic deformations can occur as a result of pore volume reduction. Since the plastic deformations are expected to dominate the elastic deformations, the stress-strain relation of the matrix is assumed to be rigid-plastic, with a yielding stress σ_{pu}. If we consider the case that both τ and σ are monotonically increasing, the contact areas are always about to slide, so that (Fig. 3a)

$$\tau_p = \mu\,\sigma_{pu} \tag{1}$$

The equilibrium conditions for one particle (Fig. 3b) can be formulated as:

$$F_x = \sigma_{pu}(a_y + \mu\,a_x) \tag{2a}$$

$$F_y = \sigma_{pu}(a_x - \mu\,a_y) \tag{2b}$$

a_x and a_y being the projected contact areas, parallel and normal to the crack plane. Taking into account all particle contributions over a unit crack area, the equilibrium is described by

$$\tau = \sigma_{pu}(\Sigma a_y + \mu\Sigma\,a_x) \quad 3a)$$

$$\sigma = \sigma_{pu}(\Sigma a_x - \mu\Sigma\,a_y) \tag{3b}$$

Since Σa_x and Σa_y are functions of the crack displacements w and Δ , the equations 3a,b are the generalized constitutive equations. In order to obtain expressions for concretes with a particular strength and composition, the values of the parameters σ_{pu}, μ should be known, and Σa_x and Σa_y should be expressed as functions of the crack width w, the shear displacement Δ and the aggregate characteristics.
The matrix yielding strength σ_{pu} must have a direct relation with the uniaxial concrete compressive strength f'_{cc}. Although no adequate data are found in literature concerning this relation, it can be expected that the value σ_{pu} is higher than the uniaxial compressive strength f'_{cc} , because this value f'_{cc} is limited by progressive microcracking between particles and matrix and not by the matrix strength.
Also about the coefficient of friction μ no specific data are found in the literature. An indication is given by tests of Weiss [5], who found for concretes and concrete components (aggregates, mortars) values, ranging from 0.4-0.6.
The projected contact areas Σa_x and Σa_y depend on both the displacements between the crack faces and the concrete mix composition, particularly the volume fraction of the aggregate particles and their grading curve. If it is assumed that the central crack line is straight, the aggregate particles are spherical (Fig. 2) and the distribution of the particles over the volume is random, the most probable values of Σa_x and Σa_y can be found by a statistical analysis. The expressions for Σa_x and Σa_y are derived in [6].

Experiments

Tests have been carried out for two reasons: to find out if the theoretical model makes sense anyhow and, if it does, to establish the expressions for σ_{pu} and μ.
The set-up of the tests is represented in Fig. 4. The specimens were precracked before actual testing. Crack opening during the actual shear test was counteracted by external restraining bars, clamping the two specimenhalves together.

The displacements between the crack faces, both in normal and parallel direction were recorded by two combinations of displacement gauges at both sides of the specimen. Variables were:

- the concrete strength: f'_{cc} = 13, 35, 59 N/mm^2
- the maximum aggregate particle diameter: D_{max} = 16, 32 mm
- the concrete type: normal, lightweight
- the initial crack width: w = 0.01, 0.20, 0.40 mm
- the stiffness of the external restraining system

All the concrete mixes were composed according to ideal Fuller curves.

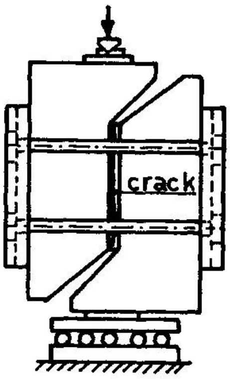

Fig. 4. Specimen with external restraining bars for tests on cracks in plain concrete

Results

For all the concrete mixes the grading curve (Fuller), the maximum particle diameter D_{max}, and the aggregate volume fraction p_k, were known. Writing the constitutive equations 3a, b as

$$\tau = \sigma_{pu} \{ \Sigma a_y(p_k, D_{max}, \Delta , w) + \mu\Sigma a_x(p_k, D_{max}, \Delta , w) \} \qquad (4a)$$

$$\sigma = \sigma_{pu} \{ \Sigma a_x(p_k, D_{max}, \Delta , w) - \mu\Sigma a_y(p_k, D_{max}, \Delta , w) \} \qquad (4b)$$

the only unknown values are σ_{pu} and μ .
Apart from the theoretical relations a large number of combinations (τ,σ,Δ,w) were obtained from the tests. Comparing the theoretical with the experimental relations, it was found that excellent fitting of the curves was obtained for

$$\sigma_{pu} = 6.39\, f'^{\,0.56}_{cc} \quad (\mathrm{N/mm^2}) \qquad (5)$$

$$\mu = 0.40 \qquad (6)$$

for all the concrete mixes (except lightweight concrete). These comparisons are shown for four mixes in the Figures 5-8*).

It should be noted that only two parameters (σ_{pu},μ) are available for curve fitting, so that only two lines per diagram (f.i. for w = 1.0 mm) can actually be fitted. The fact that it turns out that automatically all the other lines fit, demonstrates the validity of the theory.

*) The agreement between theory and experiments in these figures is even slightly better than shown earlier in [6], since here a correction is applied for the elastic deformation of the concrete between the measuring points (located 50 mm from the crack to both sides) which was earlier neglected.

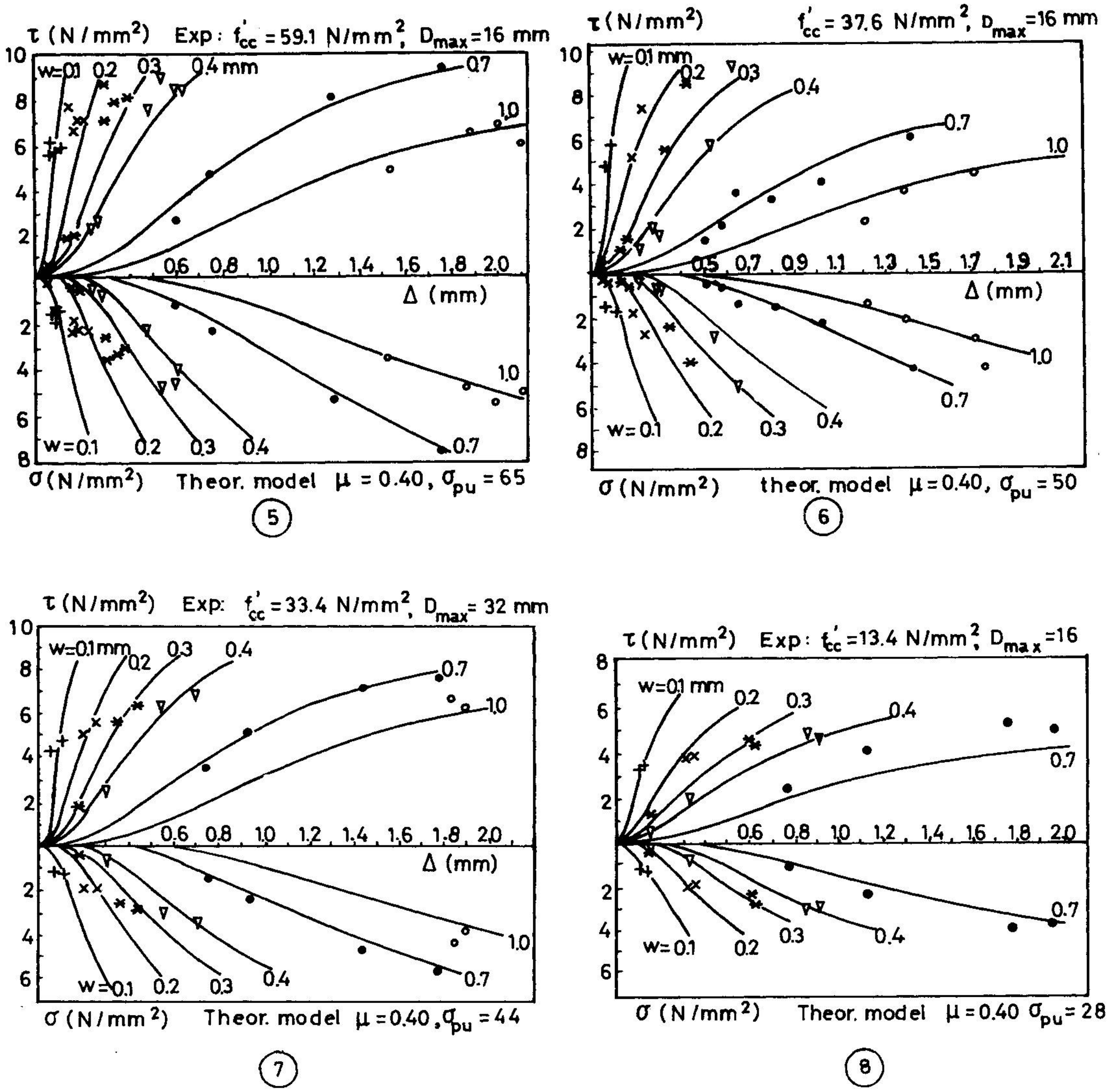

Fig. 5-8. Comparison between experimental values and theoretical lines for several concrete mixes

Fig. 5: f'_{cc} = 59.1 N/mm^2, D_{max} = 16 mm, p_k = 0.75
" 6: f'_{cc} = 37.6 " , D_{max} = 16 mm, "
" 7: f'_{cc} = 33.4 " , D_{max} = 32 mm, "
" 8: f'_{cc} = 13.4 " , D_{max} = 16 mm, "

Because τ and σ are proportional to $f'^{0.56}_{cc}$ (eq. 5) it is possible to represent the relations in a more general way. This is done in Fig. 9 and 10.

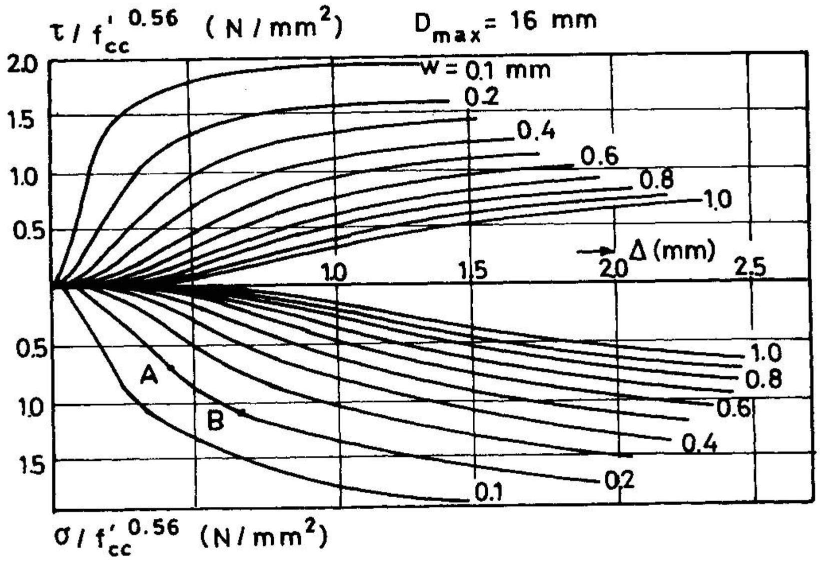

Fig. 9. Generalized constitutive relations for a crack in plain concrete ($13 < f'_{cc} < 60$ N/mm^2, D_{max} = 16 mm, p_k = 0.75)

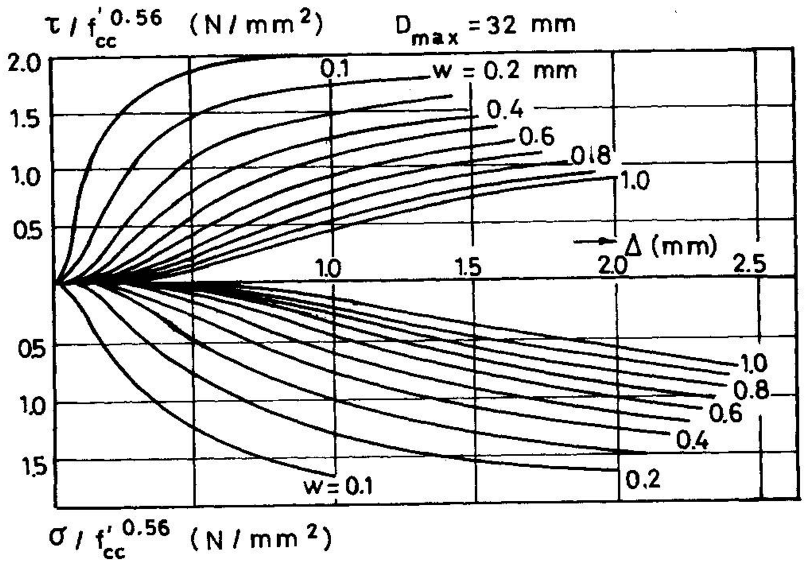

Fig. 10. The same as Fig. 9, but for $13 < f'_{cc} < 60$ N/mm^2, D_{max} = 32 mm, p_k = 0.75

Comparing both figures 9 (for D_{max} = 16 mm) and 10 (for D_{max} = 32 mm), it is seen that the differences are very small. Only for large crack widths the differences in the development of τ as a function of Δ are not insignificant. This phenomenon is also exhibited by the test (Fig. 6 and 7). The theoretical model enables a parameter study. Detailed data about this study, focussing on the influence of μ, the contribution of individual aggregate fractions, the influence of the grading curve and the behaviour under cyclic loading, are found in [6].

For the range of values tested simplified linear relations have been derived:

$$\tau = -\frac{f'_{cc}}{30} + \{1.8\, w^{-0.80} + (0.234\, w^{-0.707} - 0.20) f'_{cc}\}\Delta \quad (\tau \geq 0) \qquad (7a)$$

$$\sigma = -\frac{f'_{cc}}{20} + \{1.35 w^{-0.63} + (0.191\, w^{-0.552} - 0.15) f'_{cc}\}\Delta \quad (\sigma \geq 0) \qquad (7b)$$

(N/mm^2).
Fig. 11 shows these graphs for two of the concrete mixes.

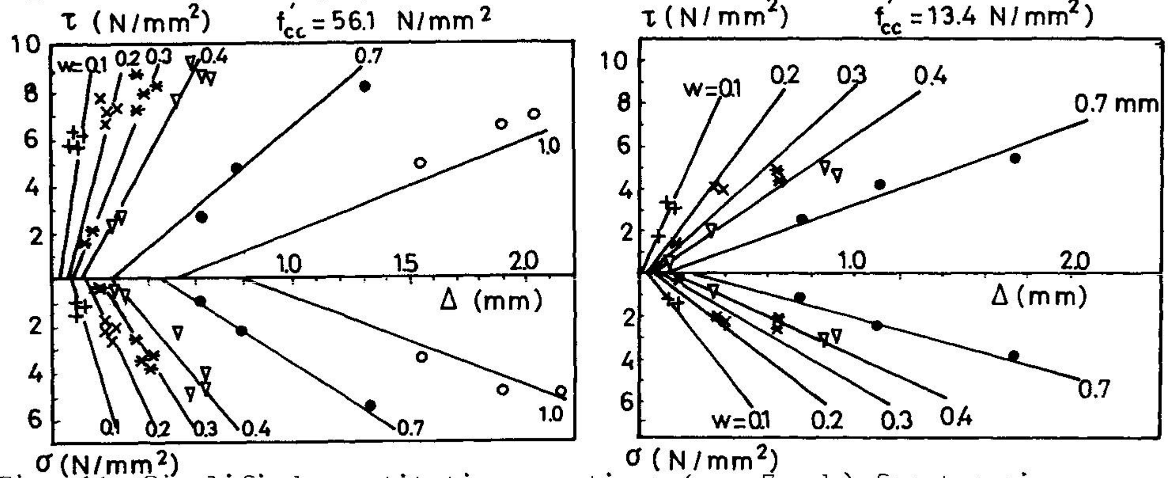

Fig. 11. Simplified constitutive equations (eq. 7a, b) for two mixes (f'_{cc} = 56.1 N/mm², left) and f'_{cc} = 13.4 N/mm², right)

2.2 Cracks in reinforced concrete

It is obvious to expect that cracks in reinforced concrete behave essentially in the same way as cracks in plain concrete, because the mechanism seems to be only slightly different: the restraining force against crack widening is not provided by an external system but internally by the reinforcing bars. The stiffness of this internal restraining system is governed by bond between bars and concrete and the yielding stress of the steel. Furtheron dowel action of the reinforcing bars is an additional component. It can however be demonstrated that, within practical limits, dowel action can be neglected without committing a significant error [6].

Experiments

Test have been carried out on specimens as represented in Fig. 12. Variables were:
- concrete strength: f'_{cc} = 20, 30-35, 56 N/mm²
- maximum particle diameter: D_{max} = 16, 32 mm
- grading curve (continuous, discontinuous)
- reinforcement ratio: ρ_o = 0.14 - 3.35%
- bar diameter
- concrete type: normal, lightweight
- inclination of the reinforcing bars (45-135° to the crack plane)

The specimens were precracked ($w \approx 0.01$-0.03 mm) and subsequently subjected to a monotonically increasing shear load. The displacements between the crack faces in normal and parallel direction were measured.
A full description is given in [7].

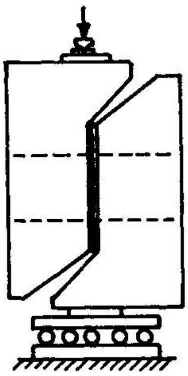

Fig. 12. Experimental set-up for tests on cracks, crossed by embedded reinforcement

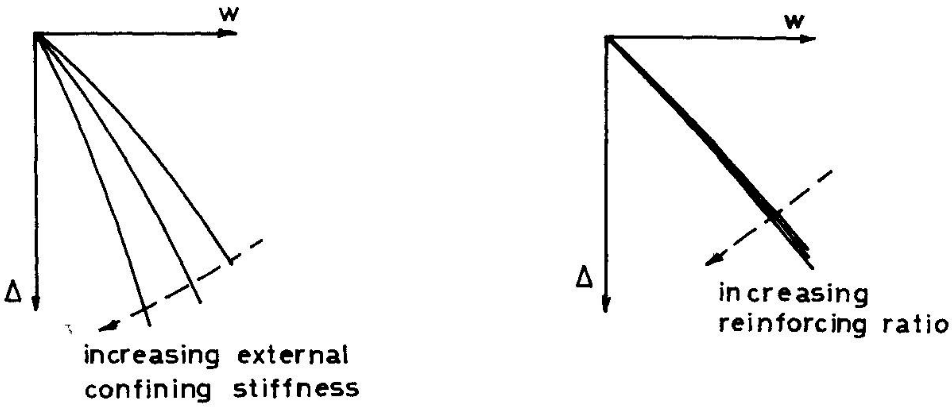

Fig. 13. Crack opening paths for cracks in plain (a) and reinforced (b) concrete with varying restraining stiffness

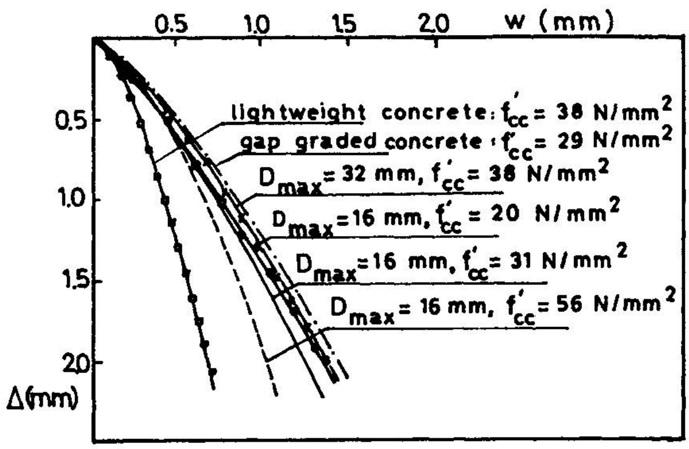

Fig. 14.

Average crack opening paths for different mixes

Results

The results of the tests on specimens with embedded reinforcement appeared to be essentially different from the results of the tests on cracks in plain concrete.
In the tests on unreinforced cracks it appeared that the external restraining stiffness has a significant influence on the crack opening path (w,Δ path). This can be shown with the aid of Fig. 9. Point A is attended with an arbitrary restraining stiffness (normal stress σ_A for a crack width $w = 0.2$ mm). If the restraining stiffness is higher ($\sigma_B > \sigma_A$ for the same crack width) this results in a larger value of Δ. So the dependency of the crack opening path on the external restraining stiffness can, in a general way, be represented as in Fig. 13a. In the tests on specimens with embedded bars the crack opening direction remained unaffected by the restraining stiffness (or reinforcement ratio) (Fig. 13b).
A similar type of behaviour was earlier reported by Mattock [8]. So, apparently the relations between stresses and displacements cannot be described on the basis of the relations derived for cracks in plain concrete (eq. 4, 5, 6) even if the restraining stiffness (load-slip relations) of the reinforcing bars were accurately known. The average crack opening paths for the different series, each of which consisted of 4 specimens of one concrete quality and reinforcement ratios of 0.56, 1.12, 1.68 and 2.23%, are represented in Fig. 14.

Four different concrete mixes with strengths of $20 < f'_{cc} < 40$ N/mm^2 displayed hardly any difference. The high strength mix ($f'_{cc} = 56$ N/mm^2) exhibited a slightly steeper crack opening path, possibly caused by breaking through of a number of the aggregate particles. The lightweight concrete showed a considerably steeper crack opening path (all lightweight particles break through). Apparently there is a fundamental difference in behaviour between unreinforced and reinforced cracks. This difference may be caused by the bond between the deformed steel and the concrete. It is known that, due to this bond, the crack width in reinforced concrete is not constant, but decreases coming nearer to the bars (Fig. 15a). It is probable that, due to this local crack width reduction higher stresses occur in the concrete around the bars, resulting in secondary cracking. In this way local compressive struts could be formed (Fig. 15b), which force the two halves of the specimen to follow a certain "cri-

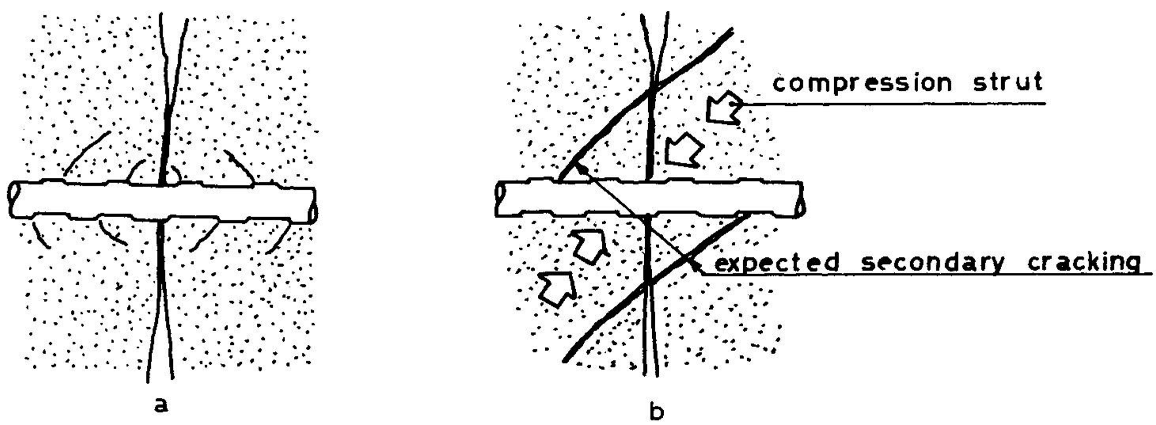

Fig 15 a. Decrease of crack width around reinforcing bar
b. formation of compression struts

tical" crack opening path. The presence of such a mechanism seems the more probable because additional tests on specimens, in which soft sleeves were secured around the reinforcing bars over a short distance to both sides of the crack, so that not such a severe crack width reduction has to be expected, displayed a behaviour similar to that of the specimens with external bars.
It turned out that the relation between τ, σ, w and Δ could be described by a model as shown in Fig. 16. Here is

F_s = the axial force in the embedded steel reinforcement (the pull-out stiffness should be known)

F_d = dowel force provided by the reinforcement. On basis of tests of other authors it was derived that the dowel force for one bar can be approximated by

$$F_d = 10(w + 0.2)^{-1} \Delta^{0.36} \phi^{1.75} f'_{cc}{}^{0.38} \qquad (\text{N, mm, N/mm}^2)$$

F_{iv}, F_{ih} = the forces due to pure aggregate interlock as described by eq. (4) or (7)

S = strut action, provided by hinged compression struts with infinite stiffness. The direction of the struts depends on the position of the crack faces (w,Δ) and is defined such that the critical w, Δ path cannot be exceeded. The struts are only active if compressed. The direction is always normal to the w,Δ path. The critical crack opening path for the concretes with $20 < f'_{cc} < 40$ N/mm^2, defined such that both the author's and Mattocks [8] tests (with large initial crack widths) could be described as

$$\frac{d\Delta}{dw} = w^{0.18} (1.65 + 2.10\, w) - 1.5\Delta \qquad (\text{mm})$$

Undoubtfully these phenomena need further study. It should be investigated if the profilation of the bars has a governing influence on the behaviour (smooth bars may be expected to give no crack width reduction and consequently to display a behaviour similar to that of external bars. Furtheron it should be studied if such type of behaviour also occurs in the case of combined shear and tension, perpendicular to the crack.

3. ULTIMATE BEARING CAPACITIES

3.1 Cracks in plain concrete

On the basis of the theory and the experiments a number of different conditions can be analysed.

3.1.a Cracks in plain concrete, not subjected to a normal compressive stress

Studying the nature of the equations (4a,b) represented in the Figs. 9 and 10, an interesting property is found: if a pair of lines for an arbitrary, constant crack width is considered, it is seen that the σ,Δ line intersects the abscis and that the τ-Δ line goes through the origin (Fig. 17). This shows that a crack can resist a shear stress even in the case that no normal compressive stress is available. For a crack width w, equilibrium is obtained for $\tau=\tau_1$, $\Delta=\Delta_1$, $\sigma = 0$.
If $\tau > \tau_1$, and the same crack width should be maintained, equilibrium can only be obtained for $\sigma > 0$: if $\sigma = 0$ an increase of the crack width (overriding of the crack faces) will occur. However, no equilibrium is possible any more (Fig. 17 $\tau_2 < \tau_1$).

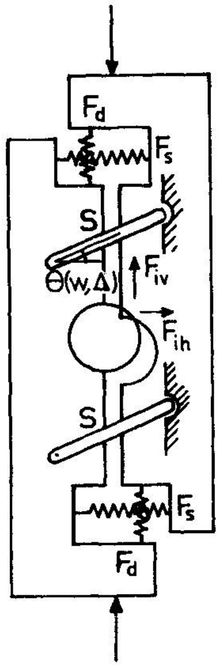

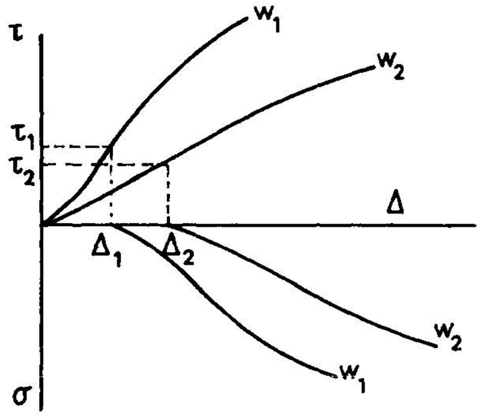

Fig. 16. Schematic representation of forces in a reinforced crack

Fig. 17.

This "stick-slip" behaviour can be explained considering the crack on particle level.
Fig. 18a shows the equilibrium condition for a small shear force: the external shear force is internally reacted by the shear and normal stresses at the contact area. If the external shear force increases, the contact area is enlarged, resulting in internal stresses which are larger but the resultant of which is inclined in another direction. The external shear force is limited due to the fact that at a certain degree a deformation, the direction of the internal reaction is turned to such an extent that no equilibrium can be obtained any more and sliding occurs (Fig. 18b).

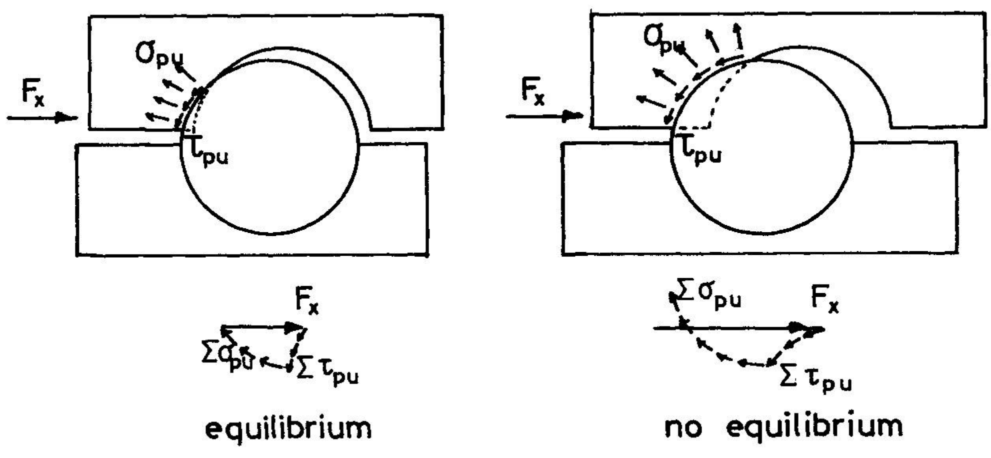

Fig. 18. Stress conditions at pure shear loading

Fig. 19 shows a number of results obtained in the tests with external bars (Fig. 5); the maximum shear stress τ_u was supposed to be reached at the load increment just before the external bars were observed to be stressed (smallest reading σ = 0.003 N/mm²).

3.1.b Cracks in plain concrete, the widening of which is prevented

Fig. 9 and 10 show that, theoretically, a maximum shear stress level is reached for every crack width. This maximum is reached if the maximum total contact area is reached (Fig. 3).
Due to the set-up of the tests, permitting an increase of the crack width during loading, no values were available to control the ultimate shear level, reached for constant crack widths. Therefore the theoretical values (Figs. 9,10) have been compared with the results of tests carried out at the TU-Munich [9]. Fig. 20 represents this comparison. It turned out that the theoretical lines (for D_{max} = 16 mm) are slightly conservative compared with the experimental values (D_{max} = 8-16 mm).

3.1.c Cracks in plain concrete, subjected to a normal compressive stress

If a crack, after opening, is subjected to a normal compressive stress , it will not close perfectly. Basing oneself on a residual value of w = 0.1 mm, the ultimate shear stress τ_u can be read as a function of the normal compressive stress in the diagrams of the Figs. 9 and 10. Fig. 21.a shows the theoretical function, compared with a number of experimental results. The values of the coefficient of friction for the crack on macro-scale $\mu_e = \tau/\sigma$ are represented in Fig. 21b. It is shown that μ_e decreases with increasing values of the normal compressive stress.

3.2. Cracks in reinforced concrete

The ultimate resistance of cracks in reinforced concrete, subjected to shear loading, has been discussed many times and several expressions for the bearing capacity have been suggested [10,11,12]. It is striking that in these expressions only a subordinate role has been attributed to the concrete strength, whereas the previous analysis of the mechanism demonstrates that the matrix strength (directly related to the concrete strength) is one of the most important variables.
The expression which is most frequently used, providing a lower bound is

$$\tau_u = 1.4 + 0.8\, \rho f_{sy} \qquad (N/mm^2) \tag{10}$$

with

$$\tau_u < 0.3\, f'_{ccyl}$$

which is known as the "modified shear-friction equation".
The concrete strength has here only been used as an upper limit, but not as an influencing variable for lower values of ρf_{sy}.

Fig. 21a showed a curve for an unreinforced crack, subjected to an external compressive stress. If reinforcement is applied, the force which is developed in the bars acts roughly in the same way: it prevents the crack from opening. However, there are a number of differences which should be noted:

- whereas in an unreinforced crack the confining stress acts to close the crack, in a reinforced crack the maximum restraining force is only reached at yielding of the steel, at a considerably larger crack width.

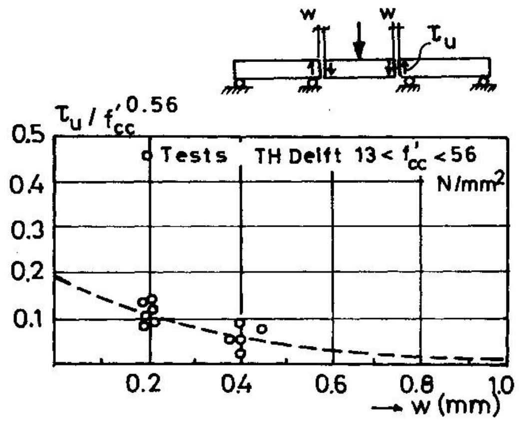

Fig. 19. Shear resistance of an unreinforced crack not subjected to any external normal force

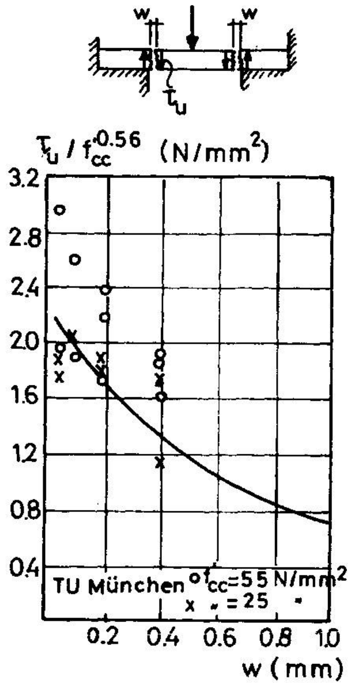

Fig. 20. Shear resistance of an unreinforced crack, the widening of which is prevented

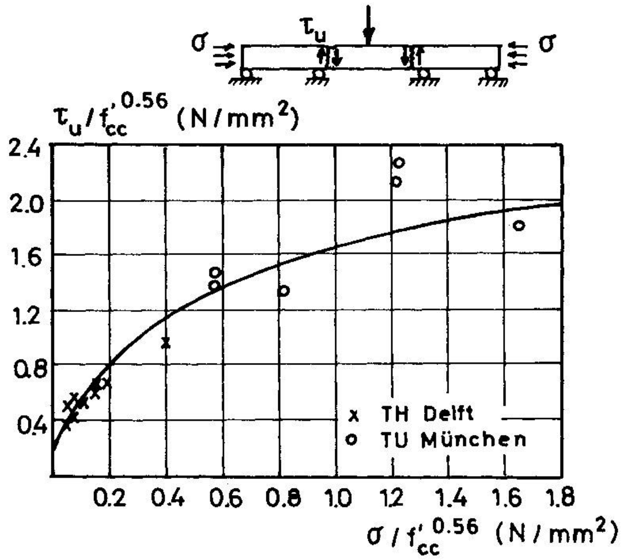

Fig. 21a. Shear resistance of an unreinforced crack, subjected to a normal compressive stress

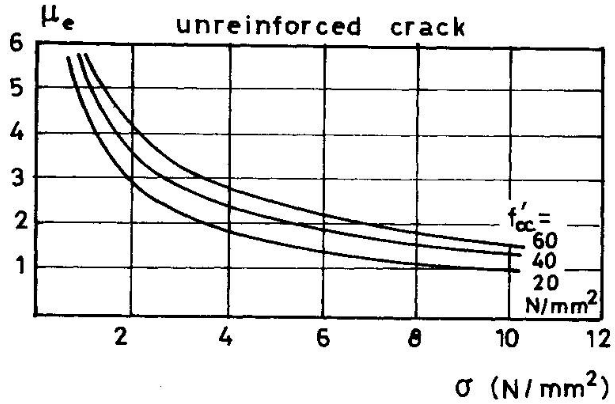

Fig. 21b. Effective coefficient of friction of an unreinforced crack

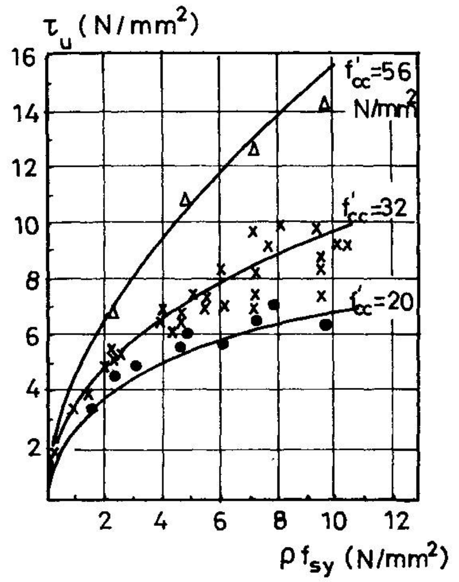

Fig. 22. Shear resistance of a reinforced crack

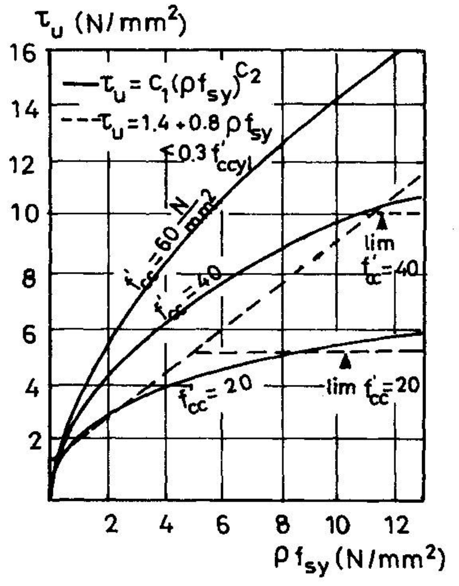

Fig. 23. Comparison between lower bounds according to eq. (10) and (12)

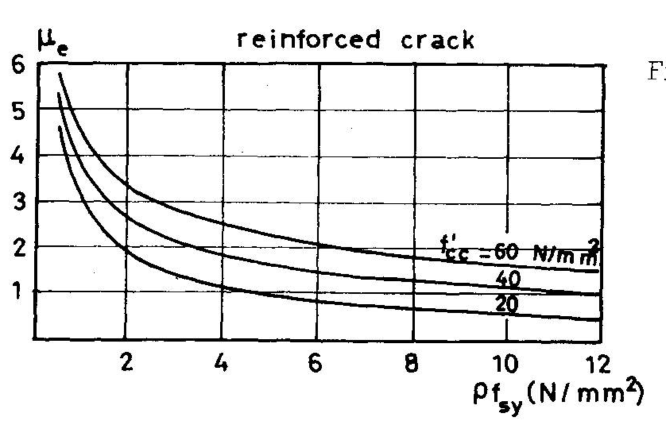

Fig. 24. Effective coefficient of friction for a reinforced crack

- as it was demonstrated before, there is a fundamental difference between the behaviour of unreinforced and reinforced cracks, probably due to crack width reduction (Fig. 15). However, the utmost part of the shear is still transferred across the crack via the contact areas between particles and matrix [6].

An increase of the concrete strength may be expected to have a positive influence on the shear resistance for three reasons:

- the matrix strength is enlarged so that a greater resistance against deformation of the crack faces is obtained.
- better bond between bars and concrete causes yielding at a smaller crack width [13] so that a larger potential contact area is available.
- by virtue of the increase of the shear resistance, resulting from the two previous points, the transverse stresses on the reinforcing bars will be larger, improving again the bond characteristics: a greater pull-out stiffness is obtained, which results in a secondary reduction of the crack width at yielding.

It seems to be realistic to assume that the relation between the ultimate shear stress τ_u and the restraining normal stress ρf_{sy} is of comparable shape as the relation between τ_u and σ for an unreinforced crack (Fig. 21a). In a generalized way this relation can be expressed as:

$$\tau_u = c_1(\rho f_{sy})^{c_2} \quad (N/mm^2) \qquad (11a)$$

where c_1 and c_2 are constants, defining the exact shape and position. For the previously discussed reasons c_1 and c_2 may be expected to be primarily functions of the concrete strength f'_{cc}. An analysis of the own results (28 tests) and a number of tests carried out by Mattock (21 tests - series 2, 3, 4, 5 [14]) showed that good agreement is obtained for

$$c_1 = f'^{0.36}_{cc} \quad (N/mm^2) \qquad (11b)$$

$$c_2 = 0.09\ f'^{0.46}_{cc} \quad (\ "\ ) \qquad (11c)$$

The average value of $\tau_{u,exp}/\tau_{u,th}$ for the 49 tests (all normal weight concrete) was 0.98 with a standard deviation of 0.10 (Fig. 22). So a 5%-lower bond is obtained with

$$\tau_u = 0.85\ c_1(\rho f_{sy})^{c_2} \quad (N/mm^2) \qquad (12)$$

Fig. 23 displays a comparison between the lower bounds according to the "modified shear friction equation" (10) and the improved equation (12). It is seen that the "modified shear friction equation" is rather conservative for higher concrete strengths. The use of (12) could result in a saving of up to 50 % of the reinforcement.
Fig. 24 shows the effective coefficient of friction μ_e based on eq. (11). It is seen that the lines are lower than the comparable ones for unreinforced cracks.
As was argued before the stress condition in the specimens is important. This was confirmed by comparing the equation (11) with the results of "pull-off" specimens, where tensile stresses instead of compressive stresses are acting perpendicular to the bars (Mattock [10], series 8, 6 tests). The average value of $\tau_{u,exp}/\tau_{u,th}$ (eq. 9) was indeed only 0.77, which can be explained by worse bond behaviour of the reinforcing bars.

4. CONCLUSIONS

- The transmission of shear and normal stresses across cracks in plain concrete can be explained on the basis of the behaviour on particle level. Constitutive equations can be derived, based on physical considerations, taking into account all concrete mix properties.
- There is a fundamental difference in behaviour between cracks in plain concrete and cracks in reinforced concrete.
- The shear-friction equations as actually used in practive give too conservative results for high strength concretes. An improved formulation for the shear resistance can be derived taking account of the concrete strength f'_{cc} and the mechanical reinforcement ratio ρf_{sy}.

5. NOTATIONS

a_x, a_y	projected contact areas parallel and normal to the crack
f'_{cc}	cube crushing strength (150 mm^3)
f_{sy}	yielding stress of the steel
p_k	volume fraction of the aggregate
w	crack width
D_{max}	maximum particle diameter
ρ	reinforcement ratio
μ	coefficient of friction (particle-matrix)
μ_e	effective coefficient of friction (crack on macro scale)
σ	stress normal to crack
σ_{pu}	matrix yielding stress
τ	shear stress
τ_p	shear stress on particle
Δ	shear displacement
ϕ	bar diameter

6. REFERENCES

[1] ACI-Committee 349: "Criteria for reinforced concrete nuclear power containment structures", ACI-journal, Vol. I, January 1972, pp. 2-28.

[2] TAYLOR, H.P.J.: "The fundamental behaviour of reinforced concrete beams in bending and shear", ACI-Special Publication SP-42, "Shear in reinforced concrete", 1974, Vol. I, pp. 43-78.

[3] FENWICK, R.C., PAULAY, T.: "Mechanisms of shear resistance of concrete beams", Journal of the Structural Division ASCE, vol. 94, No. ST10, Proc. Paper 2325, 1968, pp. 2325-2350.

[4] WALRAVEN, J.C.: "The influence of depth on the shear strength of lightweight concrete beams without shear reinforcement", Report No. 5-78-4, May 1978, Stevin Laboratory, Delft University of Technology, The Netherlands.

[5] WEISS, R.: "Ein Haufwerkstheoretisches Model der Restfestigkeit geschädigter Betone", Dissertation TU Braunschweig 1978, pp. 37-47.

[6] WALRAVEN, J.C.: "Aggregate interlock: a theoretical and experimental analysis", Dissertation, Delft University of Technology, The Netherlands, Oct. 1980.

[7] WALRAVEN, J.C., VOS, E., REINHARDT, H.W.: "Experiments on shear transfer in cracks in concrete. Part I: Description of results", Report No. 5-79-3, January 1979, Stevin Laboratory, Delft University of Technology, The Netherlands.

[8] MATTOCK, A.H.: "Effect of aggregate type on single direction shear transfer strength in monolithic concrete", Report SM 74-2, Department of Civil Engineering, University of Washington, Seattle, Washington, August 1974.

[9] DASCHNER, F.: "Schubkraftübertragung in Rissen von Normal- und Leichtbeton", Preliminary report, TU München, March 1980.

[10] MATTOCK, A.H., HAWKINS, N.M.: "Research on shear transfer in reinforced concrete - recent research", PCI-Journal, V. 17, No. 2, March-April 1972, pp. 55-75.

[11] RATHS, C.H.: Discussion of the paper "Design proposals for reinforced concrete corbels", by A.H. Mattock, PCI-Journal, V. 22, No. 2, March-April 1977, pp. 93-98.

[12] FATTAH-SHAIKH, A.: "Proposed revisions to shear-friction provisions", PCI-Journal, March-April 1978.

[13] MARTIN, H.: "Zusammenhang zwischen Oberflächenbeschaffenheit, Verbund und Sprengwirkung von Bewehrungsstählen unter Kurzzeitbelastung", Deutscher Ausschuss für Stahlbeton, Heft 228, Berlin, 1973.

[14] HOFBECK, J.A., IBRAHIM, I.O., MATTOCK, A.H.: "Shear transfer in reinforced concrete", ACI-Journal, V. 66, No. 2, Febr. 1969, pp. 119-128.